ACS APPLIED MATERIALS & INTERFACES

Letter

www.acsami.org

h-BN Monolayer on the Ni(111) Surface: A Potential Catalyst for Oxidation

A. H. M. Abdul Wasey,[†] Soubhik Chakrabarty,[†] G. P. Das,[†] and C. Majumder*[,‡]

[†]Department of Materials Science, Indian Association for the Cultivation of Science, Jadavpur, Kolkata 700032, India

[‡]Chemistry Division, Bhabha Atomic Research Centre, Trombay, Mumbai 400085, India

ABSTRACT: The hexagonal boron nitride (*h*-BN) is traditionally considered to be inert. In sharp contrast to the inert behavior of free-standing hexagonal boron nitride (*h*-BN), we propose the catalytic property of *h*-BN monolayer on Ni(111) substrate using first-principles density functional theory investigation. The interaction of O_2 molecule with the *h*-BN/Ni(111) substrate results in nondissociative adsorption of the molecule along with elongation of the O−O bond. This can be considered as the activated state of the O_2 molecule. Further interaction of this complex viz O_2−*h*-BN/Ni(111) with an incoming CO molecule leads to the spontaneous formation of CO_2. Interestingly, the CO adsorption on the *h*-BN/Ni(111) substrate was found to be unfavorable, thereby implying the oxidation of CO selectively through Eley−Rideal (ER) mechanism.

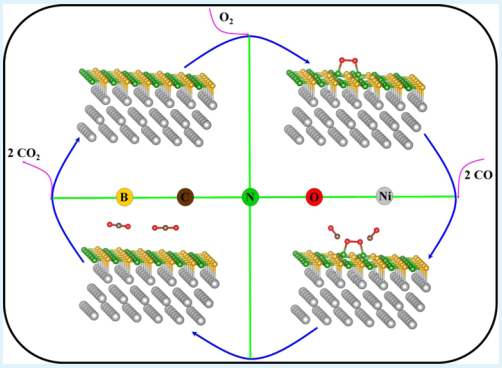

KEYWORDS: *hexagonal-BN monolayer, heterostructure, catalysis, DFT*

1. INTRODUCTION

After the discovery of graphene,[1−4] a highly promising material with its unique physicochemical properties, there has been a lot of attention given to synthesize and study its analogues. Despite the fact that hexagonal boron nitride (*h*-BN) is isostructural and isoelectronic to graphene, its electronic structure differs considerably: graphene is semimetallic and *h*-BN is wide gap insulator. The synthesis of single or few-layer *h*-BN was first carried out in ultrahigh vacuum, mostly by using borazine as the precursor and single-crystal transition metals as the substrates.[5−8] From an application perspective, synthesis of 2D nanostructure materials by exfoliation method is unlikely for scalable production. In recent times, several methods (micromechanical cleavage, liquid-phase exfoliation, and chemical vapor deposition) have been developed to prepare atomically thin *h*-BN.[8−20] Among these, CVD has shown great potential to prepare large-area *h*-BN films using borazine as precursor.

Hexagonal boron nitride is traditionally considered to be inert, preventing the adsorption of any gas molecule on it. Therefore, in recent years, several attempts have been made to functionalize the *h*-BN monolayer, which can massively expand its area of applications.[21−25] Hexagonal BN is thermally and chemically more stable than graphene and often it is used as protective coating material for transition metals.[26,27] However, the efficiency of coating depends on the thickness of the BN-layer. In this context, it is envisaged that a monolayer coating of *h*-BN sheet on a transitional metal substrate could be chemically reactive. In fact when small metal clusters are encapsulated inside the boron-nitride nanocage clusters or nanotube, the composite reportedly shows interesting catalytic behavior.[26,28] One of the most interesting features of *h*-BN monolayer adsorption on transition metal surfaces is that one can grow precisely one monolayer of *h*-BN on the substrate. However, so far no attempts have been made to explore the catalytic behavior of the transition metal supported *h*-BN monolayer. Hexagonal BN has good lattice matching with Ni(111) surface. It has been successfully grown on Ni(111) surface epitaxially by thermal decomposition of borazine producing atomically sharp interface.[7,29−31] In the present work, we have investigated the CO oxidation mechanism on the *h*-BN/Ni(111) heterostructure. The primary objective of this study is to demonstrate that *h*-BN monolayer on Ni(111) surface offers the new possibility of designing materials for oxidative catalysis.

2. COMPUTATIONAL METHOD

The geometry relaxation, total energy calculations, and the electronic structure calculations have been performed using spin polarized density functional theory based code Vienna *Ab Initio* Simulation Package (VASP).[32] The exchange-correlation part is approximated by generalized gradient approximation (GGA) of Perdew, Burke, and Ernzerhof (PBE).[33] The projector augmented wave (PAW)[34] method was employed for describing the electron-ion interactions for the elemental constituents B, C, N, O, and Ni. The plane wave basis cut off was 500 eV for all the calculations performed in this work. Ionic relaxations are performed using conjugant gradient (CG) minimization method[35] to minimize the Hellman−Feynman

Received: July 4, 2013
Accepted: October 15, 2013
Published: October 15, 2013

forces among the constituent atoms with the tolerance of 0.01 eV/Å. For all the total energy calculations reported in this paper, self-consistency has been achieved with a 1×10^{-4} eV convergence. The two-dimensional Brillouin zone (BZ) of the *h*-BN/Ni(111) slab has been sampled using Monkhorst–Pack methodology.[36] To check the effect of the van der Waals (vdW) dispersion forces, we have carried out detailed investigation of this interface by using DFT-D2 method of Grimme as implemented in the VASP code. The *h*-BN monolayer on Ni(111) substrate has been modeled by supercell geometry.

3. RESULTS AND DISCUSSION

3.1. Interface Relaxation. First, we briefly describe the equilibrium interface geometry and interaction energy between *h*-BN monolayer and Ni(111) surface. Despite a large number of theoretical and experimental studies reported on this system, we have repeated this calculation to confirm the reliability of our computational approach. More importantly, this information is necessary to understand the chemical reactivity on this surface. The *h*-BN/Ni(111) interface has been modeled by placing the *h*-BN monolayer on the Ni(111) slab comprising six Ni layers. We have considered three different adsorption configurations of *h*-BN namely; (i) N on Ni, (ii) B on Ni, and (iii) both B and N are on fcc and hcp sites. The most stable configuration is obtained by comparing the total energy after relaxing all atoms. The results reveal that "N on Ni" configuration forms the most stable structure. This "N on Ni" has two possibilities viz. B on hcp and B on fcc site between which B on fcc turns out to be slightly more stable by ∼10 meV. This is consistent with previous experimental and theoretical reports.[37−39] In Table 1 we have summarized the energetics and relevant geometrical parameters for the most stable i.e. the "N on Ni" and B on fcc configuration. The binding energy of the *h*-BN monolayer on the Ni(111) surface is estimated as

$$\Delta E_B = E_{tot} - (E_{h-BN} + E_{Ni(111)})$$

where ΔE_B denotes the binding energy per *h*-BN pair, E_{tot} is the total energy of the *h*-BN/Ni(111), $E_{h\text{-BN}}$ is the total energy of the free-standing *h*-BN sheet, and $E_{Ni(111)}$ is the total energy of the clean Ni(111) slab. It is clear from this table that the incorporation of the van der Waals (vdW) correction with GGA is important for better description of the *h*-BN/Ni interface. From the most stable interface geometry, the binding energy of B–N pair on Ni(111) surface is estimated to be −0.28 eV. The optimized N–Ni distance (2.11 Å) at the interface is in fair agreement with the reported experimental values.[7,27,37−39] In addition, the Ni(111)-supported *h*-BN surface is corrugated by 0.11 Å with B atoms closer to the Ni(111) surface than N atoms. This corrugation in the *h*-BN/Ni(111) surface is also in agreement with previously reported experimental and theoretical results.[37,38]

Table 1. Interface Relaxation of *h*-BN/Ni(111) Heterostructure

XC-functional	ΔE_B[a]	μ_b[b]	d (Å)[c]	a_{BN} (Å)[d]	a_{Ni} (Å)[e]	$a_{BN\text{-}Ni}$ (Å)[f]
LDA[g]	−0.18	3.48	2.06	2.49	2.40	2.46
LDA+vdW	−0.48	3.44	2.04	2.49	2.37	2.44
GGA-PW91[h,i]	+0.03	3.62	2.17	2.51	2.47	2.51
GGA-PW91+vdW	−0.26	3.57	2.12	2.51	2.43	2.49
GGA-PBE[j]	+0.02	3.69	2.16	2.51	2.47	2.51
GGA-PBE+vdW	−0.28	3.64	2.11	2.51	2.43	2.49

[a] ΔE_B, binding energy of *h*-BN with the Ni(111) surface (unit: eV/pair of BN atoms). [b] μ_b, total magnetic moment of the system (six Ni atoms). [c] *d*, interface distance, i.e., the N–Ni distance at the interface. [d] a_{BN}, estimated lattice parameter of *h*-BN in Å. [e] a_{Ni}, estimated Ni–Ni distance in the Ni(111) surface in Å. [f] $a_{BN\text{-}Ni}$, estimated lattice parameter of *h*-BN/Ni(111) in Å. [g] LDA, local density approximation. [h] GGA, generalized gradient approximation. [i] GGA-PW91, GGA of J. P. Perdew and Y. Wang. [j] GGA-PBE, GGA of J. P. Perdew, K. Burke and M. Ernzerhof.

After establishing the interface geometry of the *h*-BN sheet on the Ni(111) substrate, we have analyzed the electronic structure of the composite. In particular, we have investigated the effect of metal support on the electronic properties of the *h*-BN monolayer. We first compare the total density of states (DOS) of the *h*-BN sheet with and without support (Figure 1a). Although the pristine *h*-BN shows an energy gap of ∼4.5 eV, after introduction of the Ni(111) substrate, the interface states appear in the gap and spin moments are induced, suggesting significant modulation in the electronic properties of the *h*-BN monolayer. This change in the electronic behavior of the supported *h*-BN layer is attributed to the interaction between 2p and 3d orbitals of N and Ni, respectively (see Figure 1c). This is indeed a manifestation of substrate induced modulation of the inert *h*-BN sheet, and we shall demonstrate below how this justifies the possibility of using it as a novel catalyst.

3.2. Interaction of O_2 Molecule with the *h*-BN and *h*-BN/Ni(111) Surface. On the basis of the above results, viz. the modulation of the *h*-BN sheet by the metal support, it is worth studying the chemical reactivity of this supported *h*-BN sheet. For this purpose, we have modeled the *h*-BN monolayer by (6 × 6) supercell supported on three-layers thick slab consisting of 108 Ni atoms (lattice parameter $a = b = 14.92$ Å). A separation of 20 Å between two slabs is kept to avoid any unphysical interaction of the adsorbate with top and bottom layers of the slab. Such large supercell of *h*-BN/Ni(111) was considered to avoid any image interaction between adsorbate O_2 molecules.

In the first step, we have identified the most stable geometry of the O_2 molecule on a free-standing *h*-BN sheet. To start with, the O_2 molecule is placed in various orientations, parallel and perpendicular, with respect to the plane of the *h*-BN sheet. In all cases, after full ionic relaxation, it is found that the distance between O_2 molecule and the surface plane increases (B–O distance, up to 3.15 Å) (see Figure 2), corroborating the inert behavior of the free-standing *h*-BN sheet toward oxidation. The fact that the O_2 states remain unaffected when placed on pristine *h*-BN sheet, can be seen from its noninteracting behavior as evident from the PDOS plot (see Figure 1d).

In the next step, we have investigated the oxygen interaction with metal supported *h*-BN sheet. The starting configuration of the O_2 molecule on the *h*-BN/Ni(111) was similar to the free-standing *h*-BN sheet, and all atoms were allowed to relax. In contrast to the free-standing *h*-BN case, it is possible to adsorb O_2 on the *h*-BN/Ni(111) support. On the basis of the total energy of different optimized configurations, the most stable geometry of the O_2–*h*-BN/Ni(111) complex shows that O atoms prefer to bind with two nearest B atoms on the surface with O–B distance of 1.48 Å, as shown in panels a and c in Figure 3. Moreover, it is seen that the adsorption of O_2

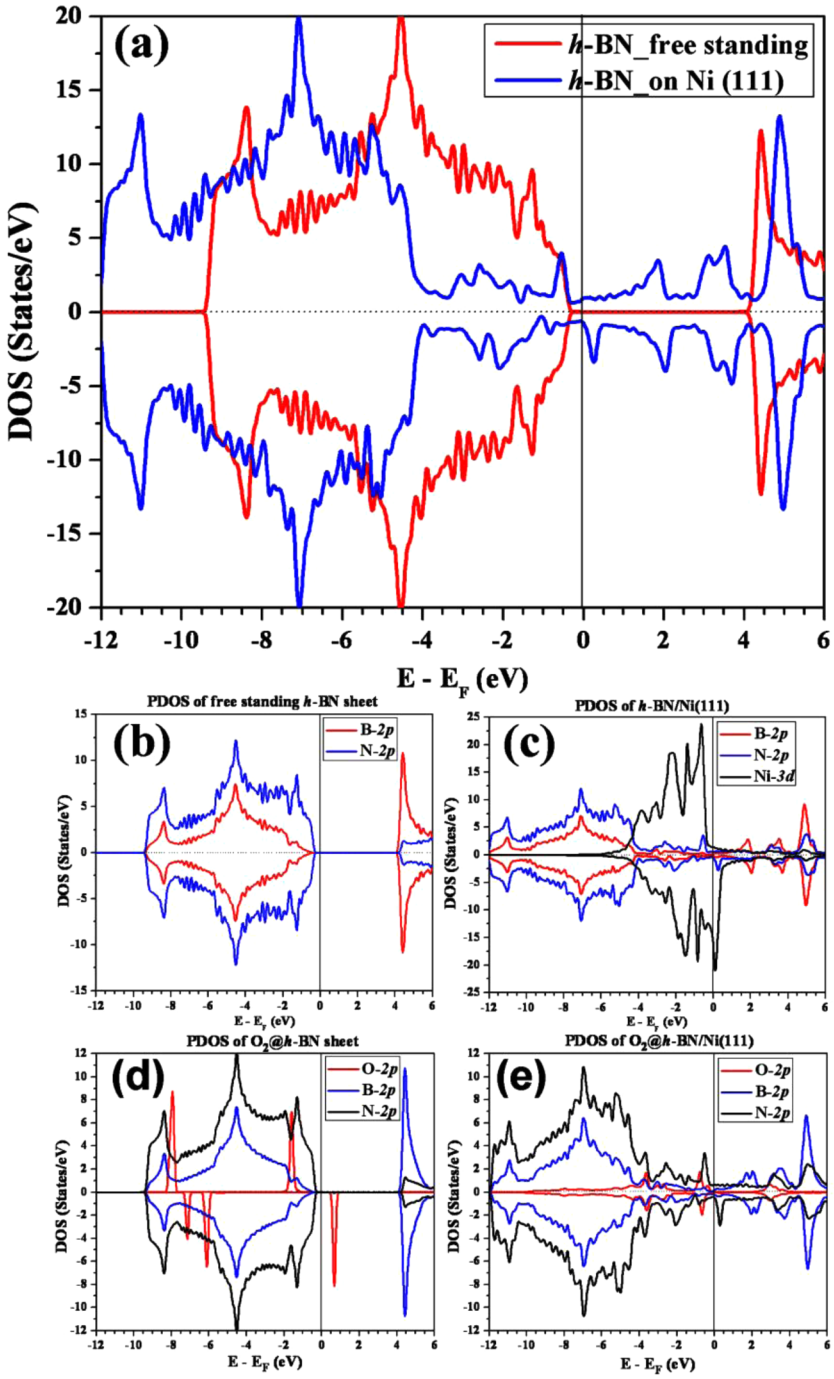

Figure 1. (a) Total DOS of free-standing and supported *h*-BN sheet. Supported *h*-BN becomes metallic as well as magnetic because of the influence of Ni. (b) Site and orbital projected DOS (PDOS) of free-standing *h*-BN sheet and (c) *h*-BN/Ni(111) showing the hybridization between B-2p and N-2p and also between N-2p and Ni-3d that is responsible for the N−Ni bonding at the interface. Here intensity of Ni-*3d* has been reduced by a suitable factor in order to compare the salient feature of its DOS and that of B-2p and N-2p. Projected DOS of O_2 on *h*-BN surface, (d) for free-standing *h*-BN and (e) Ni-supported *h*-BN.

molecule on the modulated *h*-BN sheet is associated with structural modification, i.e., B atoms bonded with the O_2 molecule are protruding out from the surface. This is depicted in the Figure 3b by zoomed view. Most importantly, the O−O bond of the adsorbed molecule is elongated up to 1.51 Å. This is significantly larger than the equilibrium O−O bond length of 1.23 Å. Thus it is inferred that O_2 molecule is activated by adsorbing on the *h*-BN/Ni(111) substrate, leading to weakening of the O−O bond. From the bond length criteria, the extent of O−O bond elongation is similar to peroxo state, a signature of activated O_2 molecule. This is further corroborated by comparing the projected density of states of O_2−*h*-BN and O_2−*h*-BN/Ni as shown in panels d and e in Figure 1. It is clear from these figures that while the energy states of O_2 retains its identity on the free-standing *h*-BN, they are merged with the *h*-BN/Ni(111) surface. This is attributed to the induced spin polarization of the *h*-BN sheet on the Ni(111) support as shown in Figure 3d. The blue and pink surfaces correspond to up and down spin magnetization respectively. The binding energy of O_2 molecule with *h*-BN/Ni(111) support is

dx.doi.org/10.1021/am404321x | ACS Appl. Mater. Interfaces 2013, 5, 10404−10408

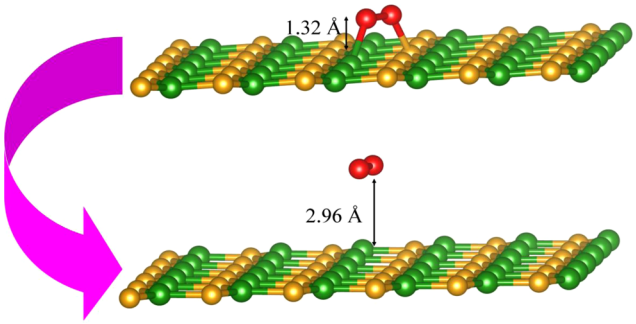

Figure 2. Interaction of O_2 molecule with a free-standing *h*-BN sheet (yellow, green, and red balls represent N, B, and O atoms respectively). After minimizing "forces", the O_2 molecule is found to move away from the surface, corroborating the inert behavior of the *h*-BN monolayer.

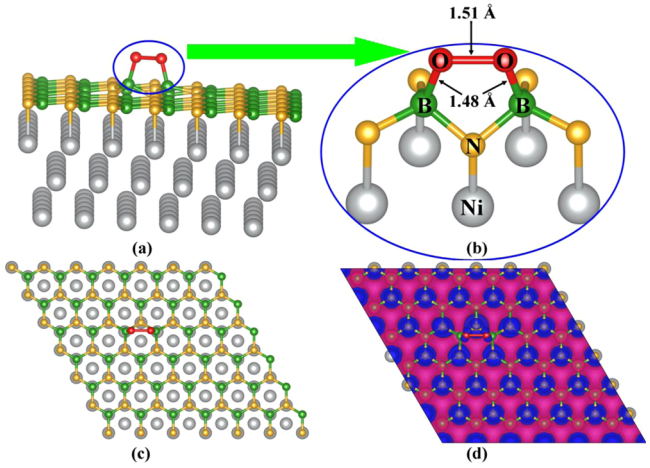

Figure 3. (a) Adsorption of O_2 molecule on the *h*-BN/Ni(111) surface. (b) Zoomed view of the topology of the bonding at the interface showing that absorption of oxygen is associated with the pulling out of B atoms from the *h*-BN surface. (c) The top view of the adsorbed O_2 molecule on *h*-BN/Ni(111) surface. (d) Spin density isosurface plot of O_2@*h*-BN/Ni(111) for isovalue ±0.0005 e/Å^3. Blue and pink surface represent spin density corresponding to up-spin and down-spin channel.

estimated to be −1.87 eV, which is large enough to weaken the O−O bond strength

$$\Delta E_B = E_{tot} - (E_{h-BN/Ni(111)} + E_{O2})$$

where ΔE_B denotes the binding energy per O_2 molecule, E_{tot} is the total energy of the system, $E_{h\text{-BN/Ni(111)}}$ is the total energy of *h*-BN/Ni(111), and E_{O2} is the total energy of free O_2 molecule.

3.3. Interaction of CO with the Preoxygenated *h*-BN/Ni(111) Surface. So far our study has revealed that an inert *h*-BN monolayer on the Ni(111) surface is chemically reactive, which can activate the oxygen molecule by transferring electronic charge to the antibonding orbital leading to weakening of the O−O bond. This suggests that *h*-BN/Ni(111) is a potential material for oxidative catalysis. To verify this proposition, we have carried out a prototype CO oxidation study, that has considerable bearing on catalytic conversion in automobile exhaust systems. The oxidation of the CO molecule occurs either by (i) Eley−Rideal (ER) or (ii) Langmuir−Hinshelwood (LH) mechanism. To investigate the CO oxidation through the ER mechanism, we have allowed a CO molecule to react with the preadsorbed O_2 molecule on the *h*-BN/Ni(111) surface (see panels a and b in Figure 4 for initial

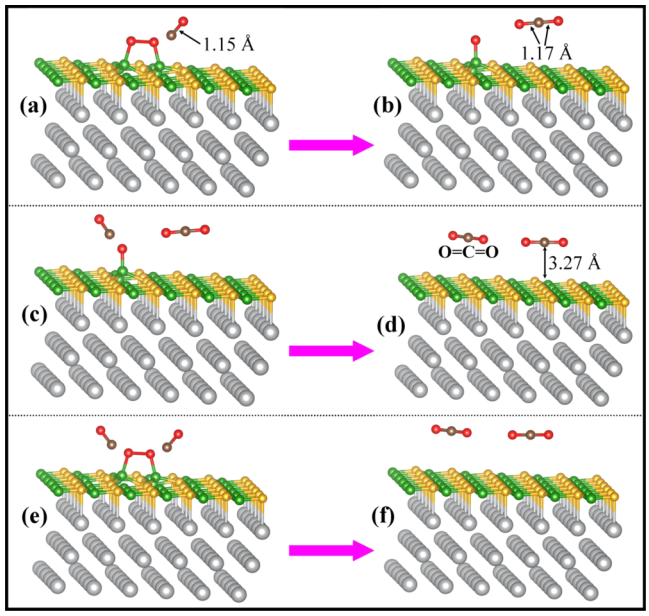

Figure 4. Typical representative figures showing the steps followed for the CO-oxidation reaction on the *h*-BN/Ni(111) composite. (a) Initial configuration of a CO molecule approaching with the preadsorbed O_2 on the *h*-BN/Ni(111) surface.(b) After geometry optimization, CO_2 forms and moves away from the surface, (c) another CO molecule approaches the remaining O atom on the surface, and (d) completes the second CO oxidation leaving the *h*-BN/Ni(111) as before the absorption of oxygen. (e, f) Initial and final geometries of the CO oxidation process when two CO molecules interacted with preadsorbed O_2 simultaneously.

and final geometry, respectively). After geometry optimization, it is seen that O−O bond ruptures spontaneously to form CO_2 and the other O atom remains connected on the *h*-BN surface. Energy released in this process [CO + O_2−*h*-BN/Ni(111) → O−*h*-BN/Ni(111) + CO_2] is estimated to be 2.54 eV. In a subsequent attempt, another CO molecule was placed to interact with the remaining O atom attached on the *h*-BN/Ni(111) surface as shown in Figure 4c. After the geometry is relaxed, the second CO also gets oxidized spontaneously to produce CO_2 (see Figure 4d) and the substrate *h*-BN/Ni(111) goes back to the initial structure as it was before absorbing any oxygen molecule on it. This process [CO + O−*h*-BN/Ni(111) + CO_2 → *h*-BN/Ni(111) + 2CO_2] releases 2.52 eV of energy. In the second case, we have placed two CO molecules simultaneously close to the preoxidized [O_2−*h*-BN/Ni(111)] surface as shown in Figure 4e. In this case also two CO_2 molecules produced spontaneously (see Figure 4f). The energy released in this process [2CO + O_2−*h*-BN/Ni(111) → *h*-BN/Ni(111) + 2CO_2] is found to be 5.05 eV, which is the sum of the energy released in the previous two consecutive processes.

For Langmuir−Hinshelwood (LH) mechanism, the reacting species are coadsorbed on the substrate before undergoing the reaction. This involves formation of an intermediate complex between CO and O_2 followed by desorption of the CO_2 molecule. For this we have optimized several initial configurations where CO molecules are placed close to the top layer of the *h*-BN/Ni substrate. The results show that unlike O_2, the CO molecule is not adsorbed on the *h*-BN/Ni

dx.doi.org/10.1021/am404321x | ACS Appl. Mater. Interfaces 2013, 5, 10404−10408

surface. This result indicates that for this substrate the CO oxidation via the LH mechanism is unfavorable.

To further underscore the efficiency of the catalyst surface, it is important to verify the interaction of the product CO_2 molecule with the *h*-BN/Ni(111) surface. For this, we have placed a CO_2 molecule at various orientations on the *h*-BN/Ni(111) surface and optimized the system. The results showed that CO_2 molecule moves away from the surface, leading to infer that the *h*-BN/Ni(111) substrate will remain unaffected by the product molecule after the reaction, which is an important signature of efficient catalyst material.

4. CONCLUSION

In summary, using plane wave based pseudopotential method under the spin polarized density functional theory, we have demonstrated for the first time that *h*-BN monolayer, an inert support, can be used as a novel catalyst for CO oxidation by depositing on the Ni(111) support. It is seen that the electronic properties of the *h*-BN monolayer is significantly modulated on the Ni(111) surface. Although free-standing *h*-BN does not interact with the O_2 molecule, the *h*-BN/Ni(111) prefers to adsorb the O_2 molecule by stretching the O−O bond up to 1.51 Å. The difference in the chemical reactivity of the supported and nonsupported *h*-BN is attributed to the substrate (in this case Ni(111)) induced midgap states.

AUTHOR INFORMATION

Corresponding Author

*E-mail: chimaju@barc.gov.in.

Notes

The authors declare no competing financial interest.

ACKNOWLEDGMENTS

This work has been carried out partially under the IBIQuS project, which provides support to A.H.M.A.W. S.C. is financially supported by a CSIR fellowship 09/080 (0787)/2011-EMR-I. G.P.D. gratefully acknowledges the financial support received from the Department of Atomic Energy, Government of India (DAE), for the IBIQuS project. G.P.D. also thanks the staff of the Center of Computational Materials Science at IMR for the use of Hitachi SR 11000-K2 Supercomputing facility, where part of the computations have been carried out. G.P.D. and C.M. would like to thank Prof. Y. Kawazoe for helpful discussions.

REFERENCES

(1) Novoselov, K. S.; Geim, A. K.; Morozov, S. V.; Jiang, D.; Katsnelson, M. I.; Grigorieva, I. V.; Dubonos, S. V.; Firsov, A. A. *Nature* **2005**, *438*, 197−200.
(2) Novoselov, K. S.; Geim, A. K.; Morozov, S. V.; Jiang, D.; Zhang, Y.; Dubonos, S. V.; Grigorieva, I. V.; Firsov, A. A. *Science* **2004**, *306*, 666−669.
(3) Novoselov, K. S.; Jiang, D.; Schedin, F.; Booth, T. J.; Khotkevich, V. V.; Morozov, S. V.; Geim, A. K. *Proc. Natl. Acad. Sci. U.S.A.* **2005**, *102*, 10451−10453.
(4) Castro Neto, A. H.; Guinea, F.; Peres, N. M. R.; Novoselov, K. S.; Geim, A. K. *Rev. Mod. Phys.* **2009**, *81*, 109−162.
(5) Auwarter, W.; Kreutz, T. J.; Greber, T.; Osterwalder, J. *Surf. Sci.* **1999**, *429*, 229−236.
(6) Corso, M.; Auwarter, W.; Muntwiler, M.; Tamai, A.; Greber, T.; Osterwalder, J. *Science* **2004**, *303*, 217−220.
(7) Nagashima, A.; Tejima, N.; Gamou, Y.; Kawai, T.; Oshima, C. *Phys. Rev. Lett.* **1995**, *75*, 3918−3921.
(8) Nagashima, A.; Tejima, N.; Gamou, Y.; Kawai, T.; Oshima, C. *Phys. Rev. B* **1995**, *51*, 4606−4613.
(9) Li, X.; Cai, W.; An, J.; Kim, S.; Nah, J.; Yang, D.; Piner, R.; Velamakanni, A.; Jung, I.; Tutuc, E.; Banerjee, S. K.; Colombo, L.; Ruoff, R. S. *Science* **2009**, *324*, 1312−1314.
(10) Bae, S.; Kim, H.; Lee, Y.; Xu, X.; Park, J.-S.; Zheng, Y.; Balakrishanan, J.; Lei, T.; Kim, H. R.; Song, Y. I. I.; Kim, Y.-J.; Kim, K. S.; özyilmaz, B.; Ahn, J.-H.; Hong, B. H.; Iijima, S. *Nat. Nanotechnol.* **2010**, *5*, 574−578.
(11) Paffett, M. T.; Simonson, R. J.; Papin, P.; Paine, R. T. *Surf. Sci.* **1990**, *232*, 286−296.
(12) Ngashima, A.; Tejima, N.; Gamou, Y.; Kawai, T.; Oshima, C. *Surf. Sci.* **1996**, *357*−*358*, 307−311.
(13) Shi, Y.; Hamsen, C.; Jia, X.; Kim, K. K.; Reina, A.; Hofmann, M.; Hsu, A. L.; Zhang, K.; Li, H.; Juang, Z.-Y.; Dresselhaus, M. S.; Li, L. −J.; Komg, J. *Nano Lett.* **2010**, *10*, 4134−4139.
(14) Chatterjee, S.; Luo, Z.; Acerce, M.; Yates, D. M.; Johnson, A. T. C.; Sneddon, L. G. *Chem. Mater.* **2011**, *23*, 4414−4416.
(15) Ci, L.; Song, L.; Jin, C.; Jariwala, D.; Wu, D.; Li, Y.; Srivastava, A.; Wang, Z. F.; Storr, K.; Balicas, L.; Liu, F.; Ajayan, P. M. *Nat. Mater.* **2010**, *9*, 430−435.
(16) Kim, K. K.; Hsu, A.; Jia, X.; Kim, S. M.; Shi, Y.; Hofmann, M.; Nezich, D.; Rodriguez-Nieva, J. F.; Dresselhaus, M.; Palacios, T.; Kong, J. *Nano Lett.* **2012**, *12*, 161−166.
(17) Lee, K. H.; Shin, H.-J.; Lee, J.; Lee, I.-Y.; Kim, G.-H.; Choi, J.-Y.; Kim, S.-W. *Nano Lett.* **2012**, *12*, 714−718.
(18) Song, L.; Ci, L.; Lu, H.; Sorokin, P. B.; Jin, C.; Ni, J.; Kvashnin, A. G.; Kvashnin, D. G.; Lou, J.; Yakobson, B. I.; Ajayan, P. M. *Nano Lett.* **2010**, *10*, 3209−3215.
(19) Dean, C. R.; Young, A. F.; Meric, I.; Lee, C.; Wang, L.; Sorgenfrei, S.; Watanabe, K.; Taniguchi, T.; Kim, P.; Shepard, K. L. *Nat. Nanotechnol.* **2010**, *5*, 722−726.
(20) Ismach, A.; Chou, H.; Ferrer, D. A.; Wu, Y.; McDonnell, S.; Floresca, H. C.; Covacevich, A.; Pope, C.; Piner, R.; Kim, M. J.; Wallace, R. M.; Colombo, L.; Ruoff, R. S. *ACS Nano* **2012**, *6*, 6378−6385.
(21) Lin, Y.; Williams, T. V.; Cao, W.; Elsayed-Ali, H. E.; Connell, J. W. *J. Phys. Chem. C* **2010**, *114*, 17434−17439.
(22) Zhang, Z.; Guo, W. *J. Phys. Chem. Lett.* **2011**, *2*, 2168−2173.
(23) Zhao, P.; Su, Y.; Zhang, Y.; Li, S.-J.; Chen, G. *Chem. Phys. Lett.* **2011**, *515*, 159−162.
(24) Sainsbury, T.; Satti, A.; May, P.; Wang, Z.; McGovern, I.; Gun'ko, Y. K.; Coleman, J. *J. Am. Chem. Soc.* **2012**, *134*, 18758−18771.
(25) Sun, Q.; Li, Z.; Searles, D. J.; Chen, Y.; Lu, G. M.; Du, A. *J. Am. Chem. Soc.* **2013**, *135*, 8246−8253.
(26) Nigam, S.; Majumder, C. *ACS Nano* **2008**, *2*, 1422−1428.
(27) Huda, M. N.; Kleinman, L. *Phys. Rev. B* **2006**, *74*, 075418−1−075418−6.
(28) Ghosh, S.; Nigam, S.; Das, G. P.; Majumdar, C. *J. Chem. Phys.* **2010**, *132*, 164704−1−164704−8.
(29) Rokuta, E.; Hasegawa, Y.; Suzuki, K.; Gamou, Y.; Oshima, C. *Phys. Rev. Lett.* **1997**, *79*, 4609−4612.
(30) Oshima, C.; Nagashima, A. *J. Phys.: Condens. Matter* **1997**, *9*, 1−20.
(31) Oshima, C.; Itoh, A.; Rokuta, E.; Tanaka, T.; Yamashita, K.; Sakurai, T. *Solid State Commun.* **2000**, *116*, 37−40.
(32) Kresse, G.; Hafner, J. *Phys. Rev. B* **1993**, *47*, 558−561.
(33) Perdew, J. P.; Burke, K.; Ernzerhof, M. *Phys. Rev. Lett.* **1996**, *77*, 3865−3868.
(34) Blöchl, P. E. *Phys. Rev. B* **1994**, *50*, 17953−17979.
(35) Pulay, P. *Chem. Phys. Lett.* **1980**, *73*, 393−398.
(36) Monkhorst, H. J.; Pack, J. D. *Phys. Rev. B* **1976**, *13*, 5188−5192.
(37) Muntwiler, M.; Awärter, W.; Baumberger, F.; Hoesch, M.; Greber, T.; Osterwalder, J. *Surf. Sci.* **2001**, *472*, 125−132.
(38) Grad, G. B.; Blaha, P.; Schwarz, K. *Phys. Rev. B* **2003**, *68*, 085404−1−085404−7.
(39) Che, J. G.; Cheng, H.-P. *Phys. Rev. B* **2005**, *72*, 115436−1−115436−7.